Fusion barrier distributions from quasielastic excitation function measurements in $^{16,18}O+^{120,124}Sn$ systems

Shrabani Sinha, M. R. Pahlavani, and R. Varma
Department of Physics, Indian Institute of Technology, Mumbai 400 076, India

R. K. Choudhury, B. K. Nayak, and A. Saxena
Nuclear Physics Division, Bhabha Atomic Research Centre, Mumbai 400 085, India

(Received 4 December 2000; revised manuscript received 11 April 2001; published 29 June 2001)

A representation of the fusion barrier distributions has been deduced from the back angle quasielastic scattering cross section data in $^{16,18}O+^{12,124}Sn$ reactions, measured over a wide range of bombarding energies around the Coulomb barrier. The results have been compared with coupled channel calculations using the CCDEF code to study the effects of projectile and target inelastic excitations and nucleon transfer couplings on the representation of fusion barrier distributions in these systems. The present studies bring out the importance of coupling of $2n$ pickup in the $^{16}O+^{120,124}Sn$ reactions and $2n$ stripping in the $^{18}O+^{120,124}Sn$ reactions in explaining the observed barrier distributions.

DOI: 10.1103/PhysRevC.64.024607 PACS number(s): 25.70.Bc, 25.70.Hi, 25.70.Jj

I. INTRODUCTION

It is known that the structure of the target and/or projectile play a crucial role in the fusion process. The coupled-channel treatment has been successfully employed in deciphering the mechanisms that are responsible for the experimentally observed enhancement in fusion cross sections at sub-barrier energies as compared to the one-dimensional barrier penetration model calculations [1,2]. The role of static nuclear deformations, vibrational excitation modes, and nucleon transfer channels in governing the fusion process have been demonstrated in many earlier studies [3–8]. The experimental representation of the fusion barrier distributions and their comparison with theoretical fusion model calculations have brought about a significant advancement in the understanding of fusion process in heavy ion reactions. The study of fusion barrier distributions allows a much deeper insight into the fusion dynamics, since the shape of the barrier distribution can directly be linked to the coupling of channels that are important in governing the fusion process at energies around the barrier. Theoretical model calculations based on coupled-channel formalism can be used to identify the relevant channels that are important for the fusion process.

The fusion barrier distribution is generally derived [9] by the double differentiation of the product of center-of-mass energy E and fusion cross sections $\sigma^{\rm fus}(E)$ with respect to the center-of-mass energy of the projectile

$$D^{\rm fus}(E)=\frac{1}{\pi R^2}\frac{d^2}{dE^2}(E\sigma^{\rm fus}).$$

It is now known that the dynamics of quasielastic scattering and fusion are inter-related. A representation of the fusion barrier distribution can therefore also be obtained from the first differentiation of the ratio between the quasielastic and the Rutherford excitation functions measured at backward angles [10] with respect to the energy $(D^{QE}(E)=-d[d\sigma_{QE}/d\sigma_{Ruth}]/dE)$. In this case, the quasielastic scattering cross section is defined as the sum of the elastic, inelastic, and the transfer cross sections. Systematic investigation and comparison of barrier distribution from the two methods has been extensively carried out and its limitations have been discussed in Refs. [10,11]. The general conclusion drawn is that for a single barrier the distribution of $D^{QE}(E)$ may be broader than $D^{\rm fus}(E)$. These two methods are seen to be complementary to each other in respect of their accuracy in the determination of the barrier distributions at below and above barrier energy regions.

The coupled-channel calculations, in general, require several ingredients such as the nucleus-nucleus potential parameters, the coupling strengths of the vibrational states and their excitation energies and rotational states with static deformations. In addition to these, there are choices to be made regarding various neutron and proton transfer channels to be included to explain the barrier structure in fusion barrier distributions. Only the positive Q-value transfer channels and low negative Q-value transfer channels are important in the coupling process, and these are known to play a role in explaining certain structures in the fusion barrier distributions [12]. Earlier experimental studies in $^{58}Ni+^{64}Ni$ [13–15], $^{32,36}S+^{58,64}Ni$ [16] reactions indicated the need to include the couplings to single-, pair-, and multinucleon transfer channels in order to explain the observed fusion excitation function data in these systems. Since then a number of systems such as $^{40}Ca+^{46,48,50}Ti$ [17], $^{32,36}S+^{110}Pd$ [18], $^{40}Ca+^{116,124}Sn$ [19], and $^{40}Ca+^{90,96}Zr$ [20] have been studied to derive the barrier distributions and to investigate the effects of positive Q-value neutron transfer channels. The importance of coupling to positive and negative Q-value transfer channels in determining the fusion barrier cross sections is now well established [3,18,21]. The coupling scheme involving positive Q-value channels would affect the barrier distributions in the low-energy side while negative Q-value channels are expected to modify the high-energy side of the average barrier in the barrier distributions.

Recently, measurements have been reported for more asymmetric systems such as $^{16,17}O+^{144}Sm$ [6] and $^{12,13}C+^{105,106}Pd$ [22], in which it is shown that the coupling to positive Q-value $1n$-stripping channel for ^{17}O and ^{13}C

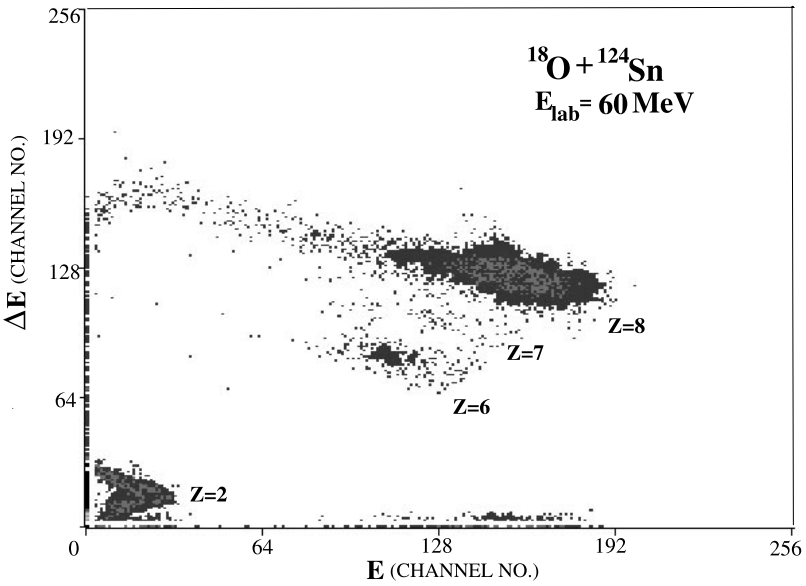

FIG. 1. A typical two-dimensional ΔE-E spectrum of reaction products in $^{18}O+ ^{124}Sn$ at 60 MeV bombarding energy.

projectiles provides a better description of the fusion barrier distributions in the low-energy region. In the case of $^{16,17}O + ^{144}Sm$ reactions, it is observed that the barrier distribution, splits into two components. This seems to be connected with the vibrational coupling to the low lying excited states in this system.

In order to investigate the effect of the positive Q-value two nucleon transfer channels on the fusion barrier distributions, we have carried out measurements for the $^{16,18}O + ^{120,124}Sn$ reactions on quasielastic scattering cross sections at backward angles. Although there is a large amount of work on the fusion barrier distributions in ^{16}O induced reactions, there are no measurements reported on fusion barrier distributions using ^{18}O projectiles. It would be of interest to investigate the strength of $2n$ transfer coupling in the ^{18}O induced reactions, since a strong coupling could lead to structures in the barrier distributions.

In the present work, the two even-even isotopes $^{120,124}Sn$ of semimagic Sn nuclei having spherical ground state shapes were chosen as the targets. The low-energy level schemes of Sn nuclei are characterized by strong vibrational quadrupole (2^+) and octupole (3^-) excitations that can be described in a theoretical approach as single phonon excitations [23–25]. One expects that in the selected systems consisting of low mass projectiles $^{16,18}O$ and medium mass targets $^{120,124}Sn$, it may be possible to isolate the effects of positive or negative Q-value transfer channels from known phonon couplings of target/projectile in the fusion barrier distributions. We have therefore aimed to focus on the role played by the transfer channels with positive Q values and low negative Q value in the determination of the fusion barrier distributions.

The paper is organized as follows. In Sec. II we describe the experimental setup and the data analysis procedure. Section III gives the discussion of the experimental results on the fusion barrier distributions as obtained from the quasielastic excitation functions and the comparison with the coupled-channel analysis. Section IV contains the summary and conclusions of the present investigations.

II. EXPERIMENTAL DETAILS AND DATA ANALYSIS

The experiments were carried out using the $^{16,18}O$ beams from the 14MV BARC-TIFR pelletron accelerator facility in

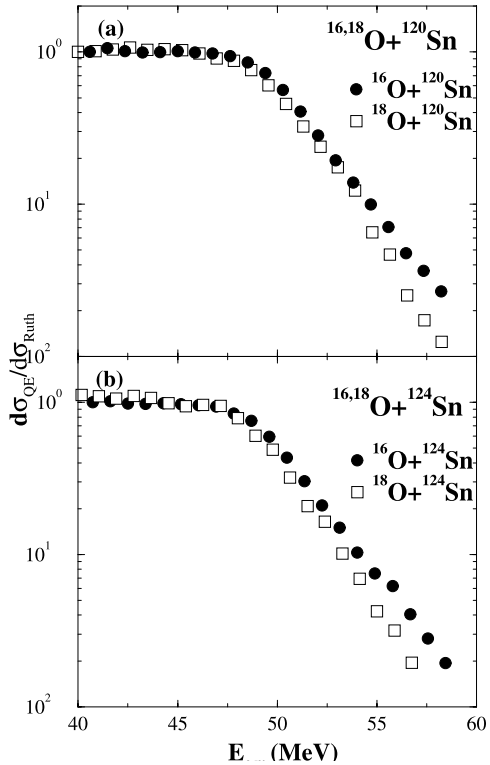

FIG. 2. Quasielastic scattering excitation functions for systems: (a) $^{16,18}O+ ^{120}Sn$ and (b) $^{16,18}O+ ^{124}Sn$.

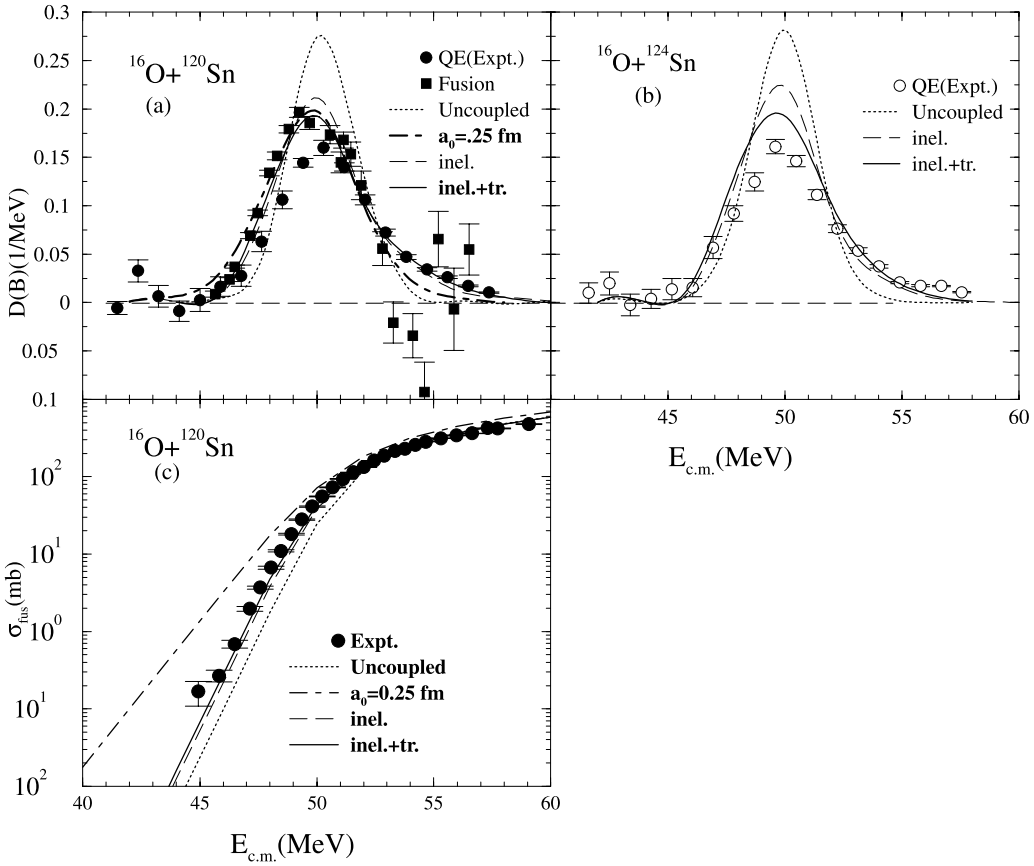

FIG. 3. (a) The experimental barrier distributions for the ^{16}O+ ^{120}Sn reaction from quasielastic excitation function data is shown as filled circles. The experimental barrier distributions derived from fusion excitation function of Ref. [29] are shown as filled squares. The dotted line is the prediction of CCDEF (uncoupled). The dot-dashed line is the prediction of CCDEF (uncoupled) with diffuseness $a_0=0.25$ fm. The dashed line is the CCDEF prediction where only single-phonon excitation of 2^+ and 3^- states of target ^{120}Sn have been included and the solid line is after further inclusion of $2n$-pickup transfer. (b) The experimental barrier distributions for the ^{16}O+ ^{124}Sn reaction are shown as circles. The dotted line is the prediction of CCDEF (uncoupled). The dashed line is the CCDEF prediction where only single-phonon excitation of 2^+ and 3^- states of target ^{124}Sn have been included and the solid line is after further inclusion of $2n$-pickup transfer. (c) The experimental fusion excitation function for the ^{16}O+ ^{120}Sn system as reported in Ref. [29] shown as filled circles. The dotted line is the prediction of CCDEF (uncoupled). The dot-dashed line is the prediction of CCDEF (uncoupled) with diffuseness parameter $a_0=0.25$ fm. The dashed line is the CCDEF prediction where only single-phonon excitation of 2^+ and 3^- states of target ^{120}Sn have been included and the solid line is after further inclusion of $2n$-pickup transfer.

Mumbai. Self-supporting targets of ^{120}Sn (500 μg/cm^2 thickness) and ^{124}Sn (400 μg/cm^2 thickness) were used in the experiment. The measurements were carried out over the bombarding energy range of $E_{lab}=42-67$ MeV in steps of 1–2 MeV intervals for both the systems. The quasielastic reaction products were measured at the backward angles using an annular gridded ionization chamber ΔE-E gas detector telescope, specially designed to carry out these measurements [26]. The anode of the detector has an active length of 15 cm and is split into two sections having lengths of 5 and 10 cm, respectively, in order to carry out the particle identification over a large range of mass and charge of the reaction products. The beam enters through the central axis of the chamber and the reaction products from the target are detected at a fixed angle in the backward direction. The reaction products from the target enter the detector through a thin entrance window provided on the front flange of the detector. The detector was placed at a distance of 15 cm from the target to cover the angular range of $\theta_{lab}=176°\pm1°$ with respect to the beam direction. The detector was operated with P-10 gas at 510 mbar pressure in order to stop the quasielastic reaction products inside its active length.

Another silicon surface barrier detector mounted at a forward angle of $\theta_{lab}=20°$ at a distance of 48 cm from the target with a collimator of 1 mm, was used to measure Rutherford scattering events for relative normalization between different runs and for the determination of the absolute cross sections. Figure 1 shows a typical two-dimensional correlation plot of ΔE-E for the ^{18}O+ ^{124}Sn reaction at $E_{lab}=60$ MeV bombarding energy. As seen from the figure quasielastic and transfer reaction products can be easily identified using this detector.

The energy integrated cross sections of the quasielastic scattering events (including transfer) as normalized to the Rutherford scattering cross sections are shown as a function of bombarding energy in Figs. 2(a) and 2(b) for ^{16,18}O

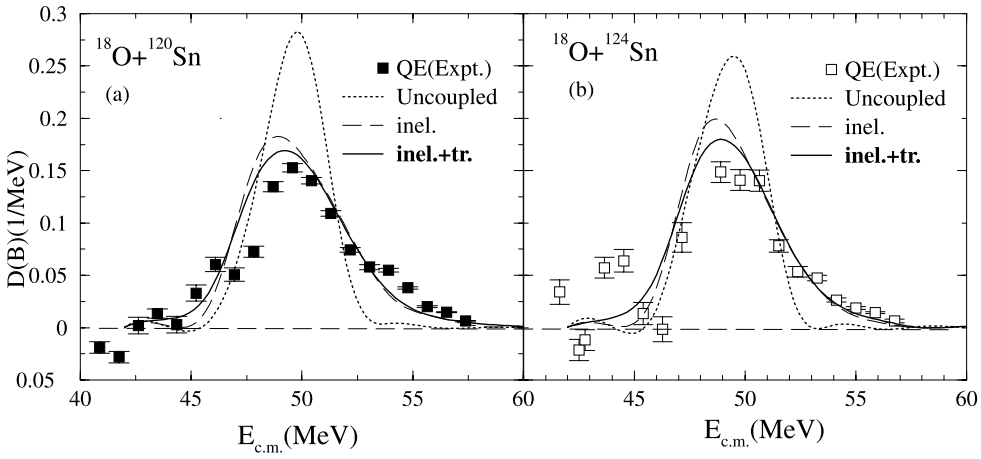

FIG. 4. (a) The experimental barrier distributions for the ^{18}O+ ^{120}Sn reaction shown as filled squares. The dotted line is the prediction of CCDEF (uncoupled). The dashed line is the CCDEF prediction where only single-phonon excitation of 2^+ and 3^- states of target ^{120}Sn and 2^+ of projectile ^{18}O have been included and the solid line is after further inclusion of $2n$-stripping transfer channel. (b) The experimental barrier distributions for the ^{18}O+ ^{124}Sn reaction shown as squares. The dotted line is the prediction of CCDEF (uncoupled). The dashed line is the CCDEF prediction where only single-phonon excitation of 2^+ and 3^- states of target ^{124}Sn and 2^+ of projectile ^{18}O have been included and the solid line is after further inclusion of $2n$-stripping transfer channel.

+ ^{120}Sn and ^{16,18}O+ ^{124}Sn reactions, respectively. It is seen that at above barrier energies the measured ratios of quasielastic to Rutherford scattering cross sections ($d\sigma_{QE}/d\sigma_{Ruth}$) are lower for the ^{18}O+ ^{120,124}Sn reaction as compared to the ^{16}O+ ^{120,124}Sn reaction.

III. FUSION BARRIER DISTRIBUTIONS

The representation of the fusion barrier distributions $D^{QE}(E)$ have been extracted from the measured quasielastic excitation functions at $\theta_{lab}=176°$ in a manner similar to that described in Refs. [27,28] and the results are shown as function of bombarding energy in Figs. 3(a) and 3(b) for ^{16}O + ^{120,124}Sn reactions and Figs. 4(a) and 4(b) for ^{18}O + ^{120,124}Sn reactions. The fusion excitation function obtained from evaporation residue measurement for ^{16}O+ ^{120}Sn system of Ref. [29] is shown in Fig. 3(c). The corresponding barrier distribution is also shown in Fig. 3(a). There is an overall agreement between the present result of barrier distribution for ^{16}O+ ^{120}Sn system derived from quasielastic measurement and that obtained from fusion excitation function measurement of Ref. [29]. It is seen from Figs. 3(a) and 3(b) and Figs. 4(a) and 4(b) that there is not much isotopic dependence of the target nuclei for the same projectile in the representation of the fusion barrier distributions in ^{16}O + ^{120,124}Sn and ^{18}O+ ^{120,124}Sn systems. The first and the second moments of the experimental barrier distributions were obtained in the energy range 45–55 MeV for various reactions as shown in Table I. It is seen from Table I, that in case of ^{18}O induced reactions, the width of the barrier distribution is larger than that of the ^{16}O induced reactions.

In order to understand the observed experimental barrier distributions more quantitatively, we have carried out the fusion coupled-channel calculation for ^{16}O+ ^{120,124}Sn and ^{18}O+ ^{120,124}Sn systems using the code CCDEF [30] without including any coupling (one-dimensional barrier penetration model). Table II gives the one-dimensional barrier potential parameters for various systems used in the CCDEF calculations. The results of CCDEF so obtained for various systems are also shown as dotted lines in Figs. 3(a) and 3(b) and Figs. 4(a) and 4(b). It is seen for all the systems that the heights of the main peak of experimental barrier distributions are lower and also the width of the barrier distributions are broader in comparison to the corresponding prediction of CCDEF without any coupling. It is expected that by decreasing the diffuseness of nuclear potential the curvature of the barrier increases, thereby increasing the width of the barrier distributions [31]. So we have matched the experimental barrier distribution for ^{16}O+ ^{120}Sn by decreasing the diffuseness parameter a_0 and adjusting the potential depth V_0 and radius r_0 of nuclear potential to get the correct barrier position V_b in CCDEF calculations. The best fit of the barrier distribution is obtained for $a_0=0.25$ fm instead of the default value $a_0=0.63$ fm. As expected, the experimental barrier distribution could be reasonably well explained by reducing diffuseness without including the couplings in CCDEF calculation. But as shown in Fig. 3(c), the corresponding fusion excitation function gets overpredicted for energies below the barrier. However, as reported in Ref. [29] by introducing channel coupling in a fusion coupled-channel model the excitation function and barrier distribution has been explained simultaneously for ^{16}O+ ^{120}Sn reaction. This is also shown in Figs. 3(a) and 3(c). Therefore, lowering the

TABLE I. First and second moments of the barrier distributions.

System	First moment	Second moment
^{16}O+ ^{120}Sn	50.6	4.71
^{18}O+ ^{120}Sn	50.1	6.19
^{16}O+ ^{124}Sn	50.2	4.92
^{18}O+ ^{124}Sn	49.9	5.29

TABLE II. The potential parameters used in the coupled-channel calculations.

System	V_b (MeV)	R_b (fm)	$\hbar\omega$ (MeV)	V_0 (MeV)	a_0 (fm)	r_0 (fm)
^{16}O+ ^{120}Sn	50.4	10.83	4.29	65.93	0.63	1.2
^{18}O+ ^{120}Sn	49.6	10.90	4.04	65.94	0.63	1.2
^{16}O+ ^{124}Sn	49.9	10.82	4.27	66.14	0.63	1.2
^{18}O+ ^{124}Sn	49.3	10.98	4.01	65.84	0.63	1.2

value of diffuseness parameter cannot explain both fusion barrier distribution and excitation function simultaneously, whereas by including channel coupling one can explain both simultaneously.

Hence, the coupled-channel calculations were carried out using the CCDEF [30] code by first including only the inelastic states of targets for the ^{16}O+ ^{120,124}Sn reactions. The single phonon 2^+ and 3^- excitations of targets ^{120,124}Sn were included in the coupled-channel analysis shown as dashed lines in Figs. 3(a) and 3(b) for ^{16}O induced reactions. The deformation parameters β_λ for different multipolarities were calculated from experimental transition strengths for various target nuclei as given in Table III.

The coupled-channel calculations including only the target excitations are not able to completely reproduce the fusion barrier distributions for the ^{16}O+ ^{120,124}Sn systems and there is still some more strength in the main peaks of the theoretical barrier distributions as shown in Figs. 3(a) and 3(b) by dashed line. This is also reflected in Fig. 3(c) where the coupled-channel calculations including only inelastic states of target ^{120}Sn shown as dashed line slightly underpredicts the excitation function at energies well below the average barrier. It is therefore necessary to introduce additional channel coupling in terms of a few nucleon transfer in the fusion coupled-channel calculations. It is known that the states with excitation energies higher than curvature of fusion barrier ($\hbar\omega$) do not affect the barrier distribution rather gives only an overall shift to the barrier position. However, in these reactions, there are no positive Q-value transfer channels. There are mostly high negative Q-value transfer channels. We have therefore included only the $2n$-pickup transfer with Q values greater than -3.5 MeV for ^{16}O + ^{120,124}Sn reactions in CCDEF. The coupled-channel calculations were performed including $2n$-pickup transfer coupling ^{120}Sn(^{16}O, ^{18}O)^{118}Sn in case of ^{16}O+ ^{120}Sn reaction and ^{124}Sn(^{16}O, ^{18}O) ^{122}Sn in case of ^{16}O+ ^{124}Sn reaction with effective Q values (Q_{eff}) as listed in Table IV. The Q value was modified to Q effective ($Q_{eff}=Q+\Delta E^C$), which is the Q value corrected by a term that takes into account the change in Coulomb energy ΔE^C caused by the transfer of particles computed according to Ref. [32]. The Coulomb barrier is given by $E_B=Z_1Z_2e^2[1-0.63/r_B]/r_B$, where $r_B=1.07[A_1^{1/3}+A_2^{1/3}]+2.72$. Only those transfer channels with $|Q_{eff}|\leqslant 3.5$ MeV and no more than two transferred nucleons of the same kind were considered. In the present calculations the value of transfer form factor has been taken as 1.0 MeV for all the systems. The results of the coupled-channel calculations including $2n$-pickup transfer channels and inelastic states of target for ^{16}O+ ^{120,124}Sn systems are shown as solid lines in Figs. 3(a) and 3(b). The calculated barrier distributions shows a closer agreement with the measured distributions when the $2n$-pickup transfer coupling is included in the CCDEF calculations.

The prediction of the CCDEF calculations with inelastic and transfer coupling on fusion barrier distributions is consistent with that derived from fusion excitation function for lower side of the average fusion barrier whereas the barrier distributions derived from quasielastic excitation function data is consistent in the higher side of the average barrier for ^{16}O+ ^{120}Sn system as shown in Fig. 3(a). Moreover, both barrier distribution and excitation function measurement for fusion are consistently explained by CCDEF calculations shown as solid line in Fig. 3(c). The inclusion of inelastic and transfer channel coupling in CCDEF calculation for ^{16}O + ^{124}Sn system also improves the agreement of its prediction with that of the experiment.

In the case of ^{18}O+ ^{120,124}Sn systems, the coupled-channel analysis was also carried out initially including only inelastic states of targets and projectile using the CCDEF code. The single phonon 2^+ and 3^- excitations of targets ^{120,124}Sn and 2^+ of projectile ^{18}O with excitation energy 1.982 MeV [33] and $\beta_2=0.355$ were included in the coupled-channel calculations and the results are shown as dashed lines in Figs. 4(a) and 4(b). The ^{18}O+ ^{120,124}Sn reactions allow for $2n$-stripping transfer channels with positive Q values. All the other transfer channels have high negative Q-value channels. The Q_{eff} values of $2n$-stripping transfer channels ^{120}Sn(^{18}O, ^{16}O) ^{122}Sn in case of ^{18}O+ ^{120}Sn reac-

TABLE III. Transition strength $B(E\lambda\uparrow)$ and deformation parameters β_λ for ^{120,124}Sn.

Nucleus	λ^π	E^*(MeV)	$B(E\lambda\uparrow)$	β_λ	Ref.
^{120}Sn	2^+	1.171	0.200×10^4 e^2 fm^4	0.137	[23,24]
^{120}Sn	3^-	2.401	0.115×10^6 e^2 fm^6	0.199	[23,24]
^{124}Sn	2^+	1.132	0.116×10^4 e^2 fm^4	0.122	[23,24]
^{124}Sn	3^-	2.614	0.073×10^6 e^2 fm^6	0.1532	[23,24]

TABLE IV. The Q_{eff} values for transfer channels included in the simplified coupled-channel calculations for each system [31].

System	Transfer channel	Q_{eff} (MeV)
^{16}O+ ^{120}Sn	$2n$-pickup	-3.1
^{16}O+ ^{124}Sn	$2n$-pickup	-1.9
^{18}O+ ^{120}Sn	$2n$-stripping	$+2.4$
^{18}O+ ^{124}Sn	$2n$-stripping	$+2.09$

tion and ^{124}Sn(^{18}O, ^{16}O)^{126}Sn in case of ^{18}O+ ^{124}Sn reaction are listed in Table IV. The results of coupled-channel analysis including $2n$-stripping transfer channels and inelastic states of projectile and target for both ^{18}O+ ^{120,124}Sn systems are shown as solid lines in Figs. 4(a) and 4(b). It is seen that compared to the earlier case with no transfer channel coupling, the height of the main peak of the barrier distributions is reduced with inclusion of the $2n$-stripping channels in the ^{18}O+ ^{120,124}Sn reactions, giving better agreement with the experimental barrier distributions.

The present study has therefore brought out the importance of transfer channel couplings on the barrier distributions in the ^{16,18}O+ ^{120,124}Sn reactions. It is shown that the coupling to the $2n$-pickup and $2n$-stripping transfer channels along with inelastic phonon couplings reproduces the overall shape of the barrier distributions in the above systems. However, peak-like structures obtained in ^{18}O induced reactions at lower side of the average barrier cannot be reproduced by calculations. So with the present data, we are not able to assign any reason to the origin of low-energy peak. Further measurements with ^{18}O induced reactions on various targets can throw more light on the origin of these structures.

IV. SUMMARY AND CONCLUSIONS

In the present work, we have carried out the quasielastic excitation function measurements of ^{16,18}O+ ^{120,124}Sn at the backward angle of $\theta_{lab}=176°$, around the respective fusion barrier energies of the systems. The representation of fusion barrier distributions for ^{16,18}O+ ^{120,124}Sn systems obtained from quasielastic excitation function measurement and also the barrier distribution for ^{16}O+ ^{120}Sn system obtained from fusion excitation function measurement of Ref. [29] are compared with the prediction of one-dimensional barrier penetration (uncoupled CCDEF) model by changing the diffuseness parameter of nuclear potential. By doing this, it is possible to explain the observed experimental barrier distribution but the excitation function gets overpredicted for energies below the fusion barrier. On the contrary, keeping the diffuseness parameter at 0.63 fm but by inclusion of couplings of 2^+, 3^- inelastic states of target nuclei in CCDEF calculations, we could explain the barrier distribution to a large extent. Moreover, the agreement could be further improved with the inclusion of two-neutron pickup transfer channels in ^{16}O + ^{120,124}Sn systems and two-neutron stripping transfer channels in ^{18}O+ ^{120,124}Sn systems. In addition, for ^{16}O+ ^{120}Sn system, the predictions of CCDEF with the inclusion of inelastic and transfer coupling explains the fusion barrier distributions and fusion excitation functions better in comparison to prediction of coupled-channel calculations with just multiphonon couplings as mentioned and shown in Ref. [29]. This work therefore, brings out the importance of transfer coupling in explaining fusion barrier distributions in these reactions.

ACKNOWLEDGMENTS

The authors would like to thank Dr. S. S. Kapoor for many helpful discussions and suggestions on this work. Thanks are also due to the Pelletron staff for their help in providing the required beams and with the accelerator operations. Two of us (S.S. and R.V.) would like to acknowledge the support of Board for Research in Nuclear Science (BRNS), Department of Atomic Energy (DAE), Department of Science and Technology (DST), and Council of Scientific and Industrial Research (CSIR), Government of India for providing financial support for this work.

[1] M. Beckerman, Rep. Prog. Phys. **51**, 1047 (1988).
[2] S. G. Steadman and M. J. Rhoades-Brown, Annu. Rev. Nucl. Part. Sci. **36**, 649 (1986).
[3] J. R. Leigh, M. Dasgupta, D. J. Hinde, J. C. Mein, C. R. Morton, R. C. Lemmon, J. P. Lestone, J. O. Newton, H. Timmers, and J. X. Wei, Phys. Rev. C **52**, 3151 (1995).
[4] D. J. Hinde, M. Dasgupta, J. R. Leigh, J. P. Lestone, J. C. Mein, C. R. Mortan, J. O. Newton, and H. Timmers, Phys. Rev. Lett. **74**, 1295 (1993).
[5] J. R. Bierman, P. Chan, J. F. Liang, M. P. Kelly, A. A. Sonzogni, and R. Vandenbosch, Phys. Rev. Lett. **76**, 1587 (1996).
[6] C. R. Morton, M. Dasgupta, D. J. Hinde, J. R. Leigh, R. C. Lemmon, J. P. Lestone, J. C. Mein, J. O. Newton, H. Timmers, N. Rowley, and A. T. Kruppa, Phys. Rev. Lett. **72**, 4074 (1994).
[7] A. M. Stefanini, D. Ackermann, L. Corradi, D. R. Napoli, C. Petrache, P. Spolare, P. Bednarczyk, H. Q. Zhang, S. Beghini, G. Montagnoli, L. Mueller, F. Scarlassara, G. F. Segato, F. Soramel, and N. Rowley, Phys. Rev. Lett. **74**, 864 (1995).
[8] C. R. Morton, A. C. Berriman, M. Dasgupta, D. J. Hinde, J. O. Newton, K. Hagino, and I. J. Thompson, Phys. Rev. C **60**, 044608 (1999).
[9] N. Rowley, G. H. Satchler, and P. H. Stelson, Phys. Lett. B **254**, 25 (1991).
[10] H. Timmers, J. R. Leigh, M. Dasgupta, D. J. Hinde, R. C. Lemmon, J. C. Mein, C. R. Morton, J. O. Newton, and N. Rowley, Nucl. Phys. **A584**, 190 (1995).
[11] N. Rowley, H. Timmers, J. R. Leigh, M. Dasgupta, D. J. Hinde, J. C. Mein, C. R. Morton, and J. O. Newton, Phys. Lett. B **373**, 23 (1996).
[12] R. A. Broglia, C. H. Dasso, and S. Landowne, Phys. Rev. C **32**, 1426 (1983).
[13] M. Beckerman, M. Salomaa, A. Sperduto, H. Enge, J. Ball, A. DiRienjo, S. Gazes, Yan Chen, J. D. Molitoris, and Mao Naifeng, Phys. Rev. Lett. **45**, 1472 (1980).
[14] M. Beckerman, J. Ball, H. Enge, M. Salomaa, A. Sperduto, S. Gazes, A. DiRienjo, and J. D. Molitoris, Phys. Rev. C **23**, 1581 (1981).
[15] M. Beckerman, M. Salomaa, A. Sperduto, J. D. Molitoris, and A. DiRienjo, Phys. Rev. C **25**, 837 (1982).
[16] A. M. Stefanini, G. Fortuna, R. Pengo, W. Meckzynski, G. Montagnoli, L. Corradi, A. Tivelli, S. Beghini, C. Signorini, S. Lunardi, M. Morando, and F. Soramel, Nucl. Phys. **A456**, 509 (1986).

[17] A. A. Sonzogni, J. D. Bierman, M. P. Kelly, J. P. Lestone, J. F. Liang, and R. Vandenbosch, Phys. Rev. C **57**, 722 (1998).
[18] A. M. Stefanini, D. Ackermann, L. Corradi, J. H. He, G. Montagnoli, S. Beghini, F. Scarlassara, and G. F. Segato, Phys. Rev. C **52**, R1727 (1995).
[19] A. M. Stefanini, J. Phys. G **23**, 1401 (1997).
[20] H. Timmers, L. Corradi, A. M. Stefanini, D. Ackermann, J. H. He, S. Beghini, G. Montagnoli, F. Scarlassara, A. M. Stefanini, G. F. Segato, and N. Rowley, Phys. Lett. B **399**, 35 (1997).
[21] R. A. Broglia, C. H. Dasso, S. Landowne, and A. Winther, Phys. Rev. C **27**, 2433 (1983).
[22] O. A. Capurro, J. E. Testoni, D. Abriola, D. E. DiGregorio, G. V. Marti, A. J. Pacheco, M. R. Spinella, and E. Achterberg, Phys. Rev. C **62**, 014613 (2000).
[23] J. Bryssinck, L. Govor, D. Belic, F. Bauwens, O. Beck, P. von Brentano, D. De Frenne, T. Eckert, C. Fransen, K. Govaert, R. D. Herzberg, E. Jacobs, U. Kneissl, H. Maser, A. Nord, N. Pietralla, H. H. Pitz, V. Yu. Ponomarev, and V. Werner, Phys. Rev. C **59**, 1930 (1999).
[24] J. Bryssinck, L. Govor, V. Yu. Ponomarev, F. Bauwens, O. Beck, D. Belic, P. von Brentano, D. De Frenne, T. Eckert, C. Fransen, K. Govaert, R. D. Herzberg, E. Jacobs, U. Kneissl, H. Maser, A. Nord, N. Pietralla, H. H. Pitz, and V. Werner, Phys. Rev. C **61**, 024309 (2000).
[25] A. Bohr and B. Mottelson, *Nuclear Structure* (Benjamin, New York, 1975).
[26] B. V. Dinesh, R. G. Thomas, B. K. Nayak, D. C. Biswas, A. Saxena, L. M. Pant, P. K. Sahu, and R. K. Choudhury, Nucl. Instrum. Methods Phys. Res. A **452**, 338 (2000).
[27] R. Varma, Shrabani Sinha, B. K. Nayak, R. G. Thomas, A. Saxena, D. C. Biswas, L. M. Pant, D. M. Nadkarni, R. K. Choudhury, and P. Bhattacharya, Phys. Rev. C **57**, 3462 (1998).
[28] Shrabani Sinha, R. Varma, R. K. Choudhury, B. K. Nayak, A. Saxena, R. G. Thomas, and B. V. Dinesh, Phys. Rev. C **61**, 034612 (2000).
[29] Lagy T. Baby, Vandana Tripathi, J. J. Das, P. Sugathan, N. Madhavan, A. K. Sinha, M. C. Radhakrishna, P. V. Madhusudhana Rao, S. K. Hui, and K. Hagino, Phys. Rev. C **62**, 014603 (2000).
[30] J. Fernandez-Niello, C. H. Dasso, and S. Landowne, Comput. Phys. Commun. **54**, 409 (1989).
[31] J. R. Bierman, P. Chan, J. F. Liang, M. P. Kelly, A. A. Sonzogni, and R. Vandenbosch, Phys. Rev. C **54**, 3068 (1996).
[32] R. A. Broglia and A. Winther, *Heavy Ion Reactions* (Benjamin, Reading, MA, 1981), Vol. 1, p. 116.
[33] S. Raman, C. H. Malarkey, W. T. Milner, C. W. Nestor, Jr., and P. H. Stelson, At. Data Nucl. Data Tables **36**, 1 (1987).